

## Supporting Information

### Multimodal bioimaging using rare earth doped Gd<sub>2</sub>O<sub>3</sub>: Yb/Er phosphor with upconversion luminescence and magnetic resonance properties

G. Ajithkumar<sup>a1</sup>, Benjamin Yoo<sup>b</sup>, Dara E. Goral<sup>b</sup>, Peter J. Hornsby<sup>b</sup>, Ai-Ling Lin<sup>c</sup>,  
Uma Ladiwala<sup>d</sup>

Vinayak P. Dravid<sup>e</sup> and Dhiraj K Sardar<sup>a</sup>

<sup>a</sup>*Department of Physics and Astronomy, University of Texas at San Antonio, San Antonio, TX 78249*

<sup>b</sup>*Department of Physiology and Barshop Institute, University of Texas Health Science Center at San Antonio, San Antonio, TX 78245*

<sup>c</sup>*Research Imaging Institute, Barshop Institute and Department of Cellular & Structural Biology, University of Texas Health Science Center, 7703 Floyd Curl Drive, San Antonio, TX 78229*

<sup>d</sup>*UM-DAE Centre for Excellence in Basic Sciences, Health Centre Bldg, University of Mumbai, Kalina Campus, Mumbai 400098*

<sup>e</sup>*Department of Materials Science and Engineering, Northwestern University, 2220 Campus Drive, Evanston, IL 60208-3108*

---

<sup>1</sup> Corresponding author email: akgsh@yahoo.com  
Fax 2104584919

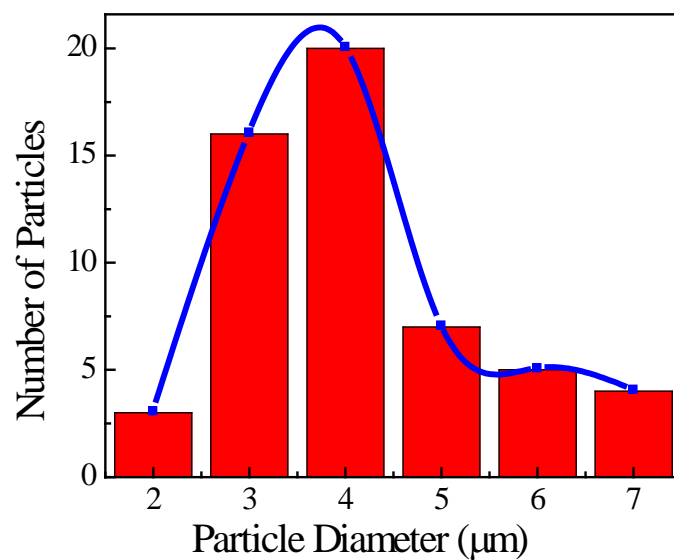


**Figure S1.** Particle size distribution obtained from SEM image analysis. Images were analyzed from different locations and the distributions obtained from over 200 particles.

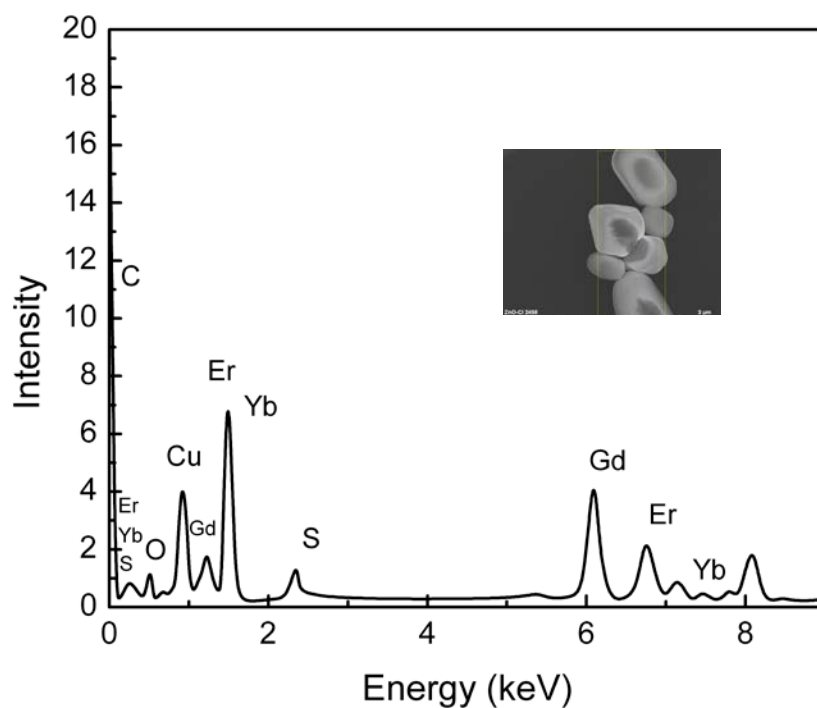


**Figure S2.**EDAX spectrum of the  $Gd_2O_2S: Yb/Er$  phosphor showing the elemental compositions. The C and Cu peaks originate from the carbon coated copper TEM grid. The inset shows the SEM image with square corresponding to the imaging location.

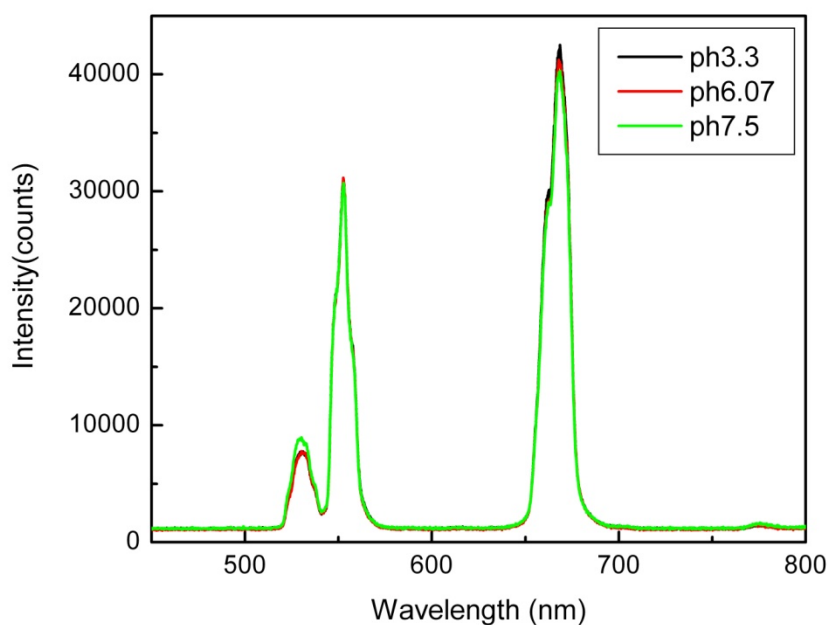


**Figure S3.**Upconversion emission spectra in  $Gd_2O_2S:YbEr$  under different pH conditions of the medium.

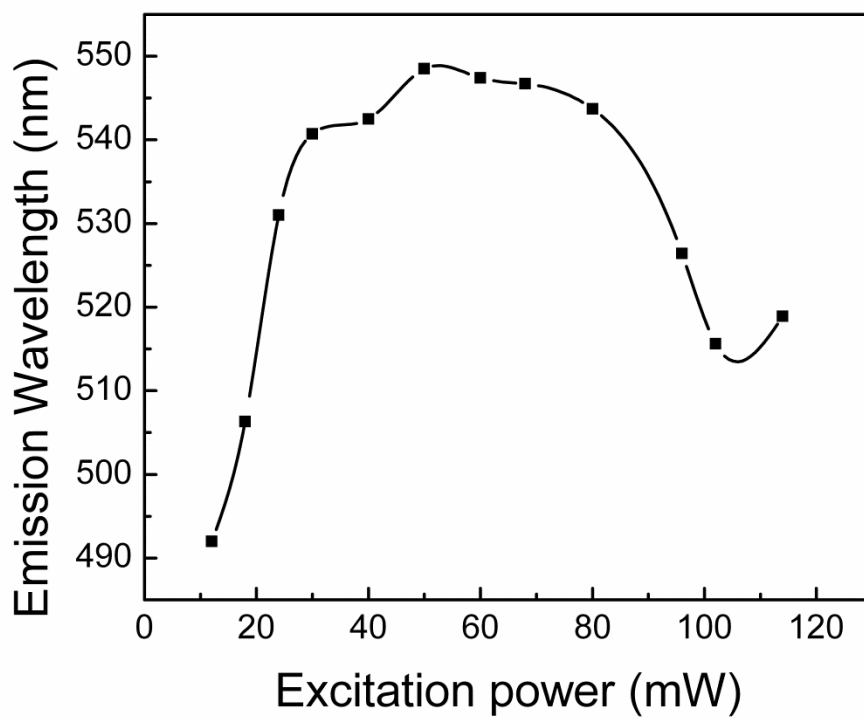


**Figure S4.** Color tuning behavior in  $\text{Gd}_2\text{O}_2\text{S: Yb/Er}$  under 980 nm laser excitation.

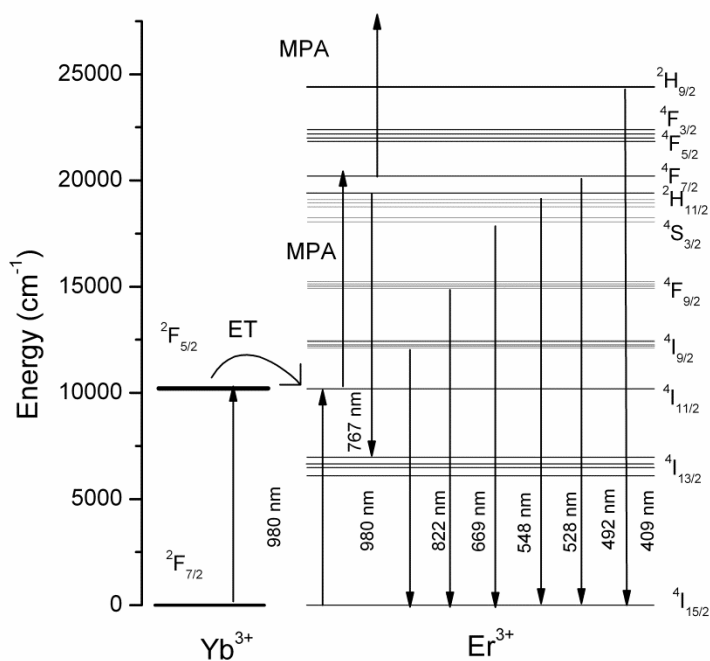


**Figure S5.** Energy level structure and excitation and de excitation mechanisms in the Gd<sub>2</sub>O<sub>3</sub>S: Yb/Er phosphor under 980 nm excitation. MPA- multiphoton absorption, ET-Energy transfer. All emission bands observed under 980 nm excitation are indicated.

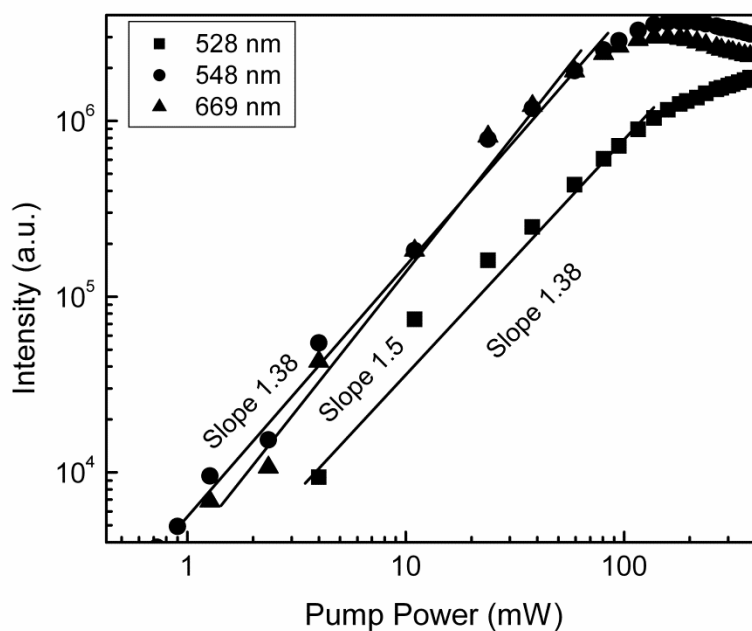


**Figure S6.** Pump power dependence of the green and red emission bands on 980 nm excitation power in  $\text{Gd}_2\text{O}_2\text{S}:\text{Yb/Er}$  phosphor.

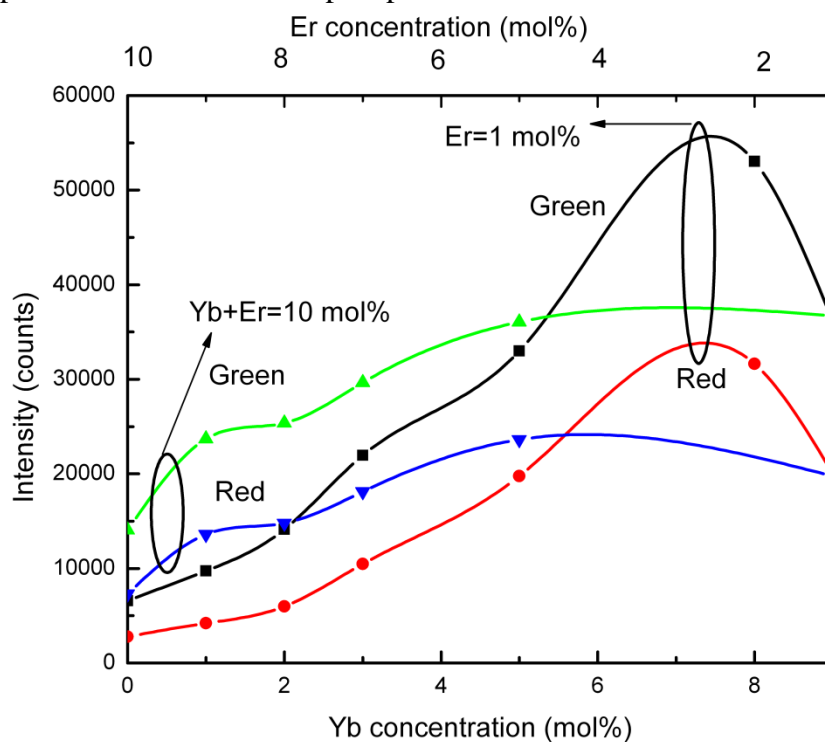


**Figure S7.** Variation of the red and green emission intensity with Yb and Er in  $\text{Gd}_2\text{O}_2\text{S}:\text{Yb/Er}$  phosphor. Top circles curves for Er =1mol% and bottom circles curves for Yb+Er =10 mol%.

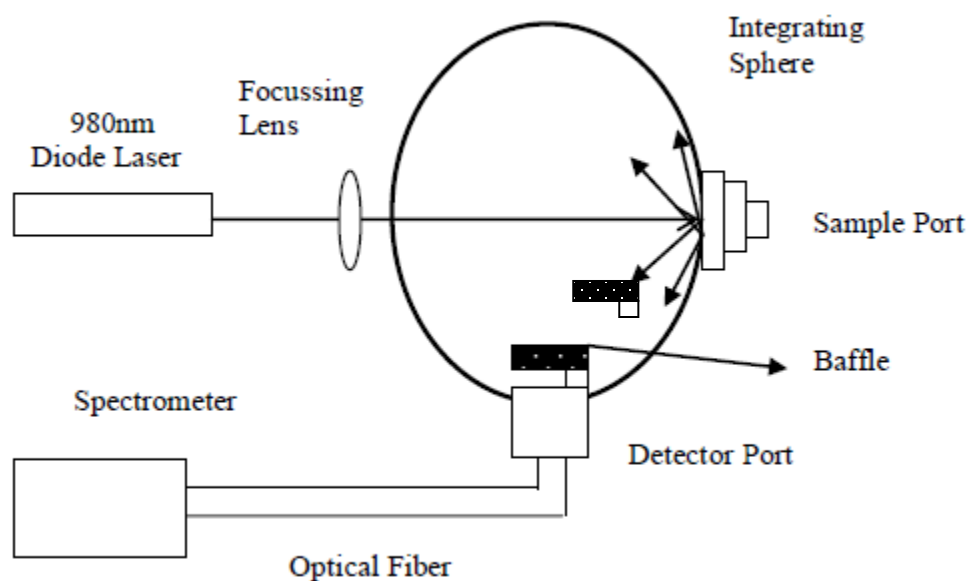


**Figure S8.** Schematic of the integrating sphere setup for measuring the quantum efficiency of the phosphor.

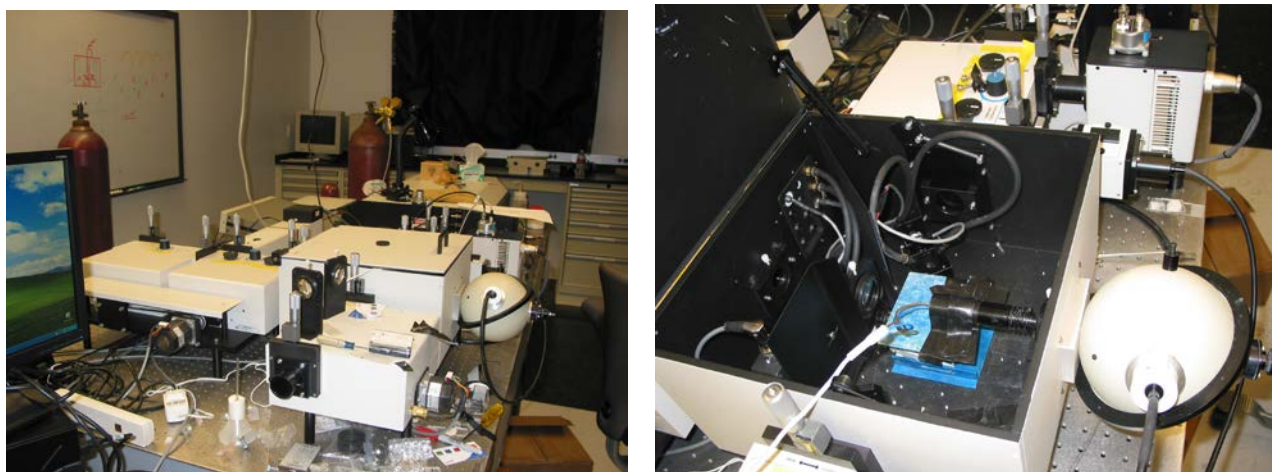


**Figure S9**(left). Photograph of the experimental setup illustrated in Figure S8. Right-Closeup view of the sphere and the diode laser inside the sample chamber.

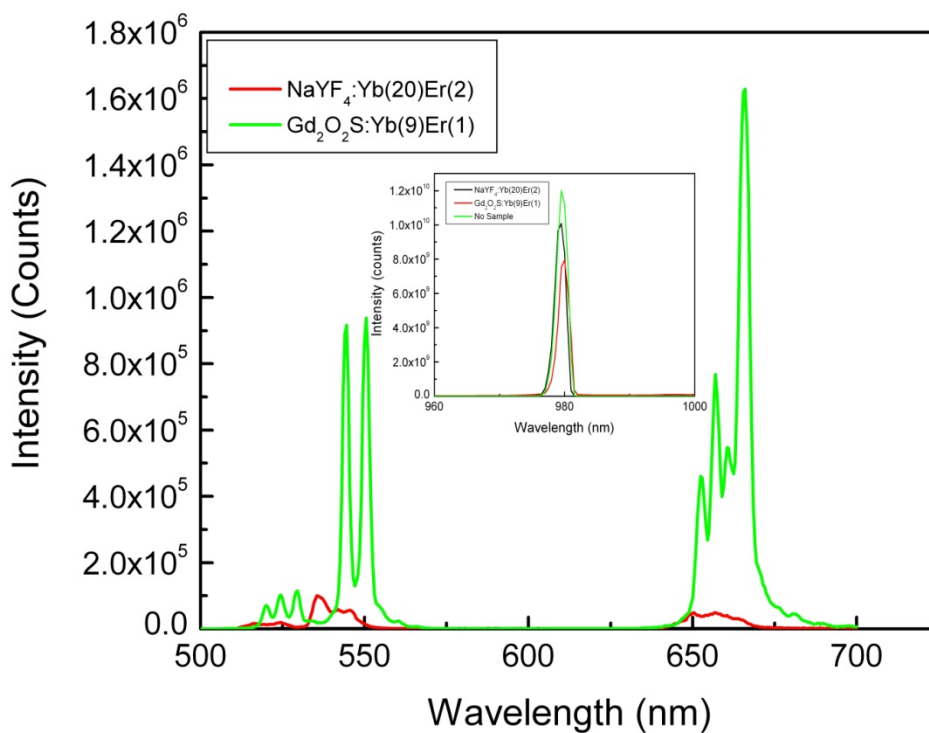


**Figure S10.** Comparison of the 980 nm excited upconversion emission spectra of NaYF<sub>4</sub>: Yb (20%) Er (2%) and Gd<sub>2</sub>O<sub>2</sub>S: Yb (9) Er (1) phosphors collected with integrating sphere under identical conditions. The inset shows the 980 nm laser excitation profile.

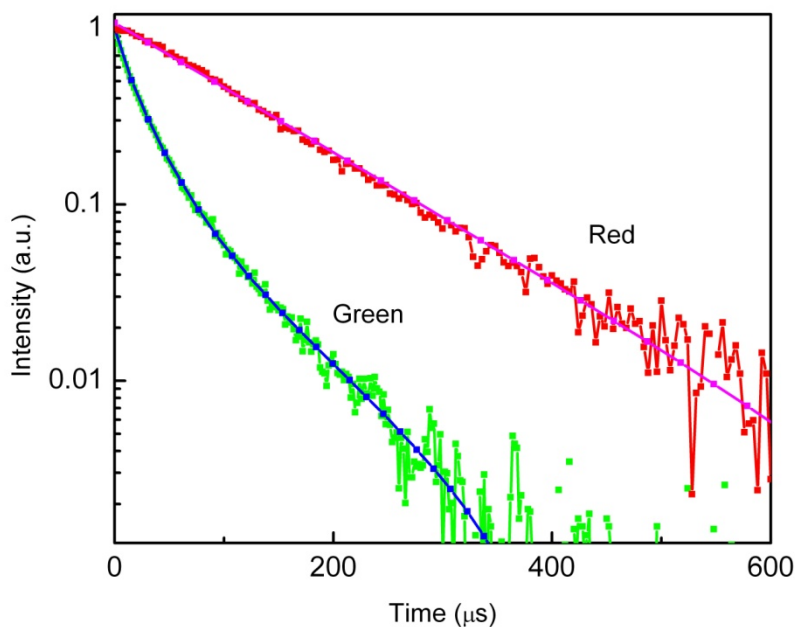


**Figure S11.** Fluorescence decay curves of the green and red emission in Gd<sub>2</sub>O<sub>2</sub>S: Yb (8) Er (1) phosphor.

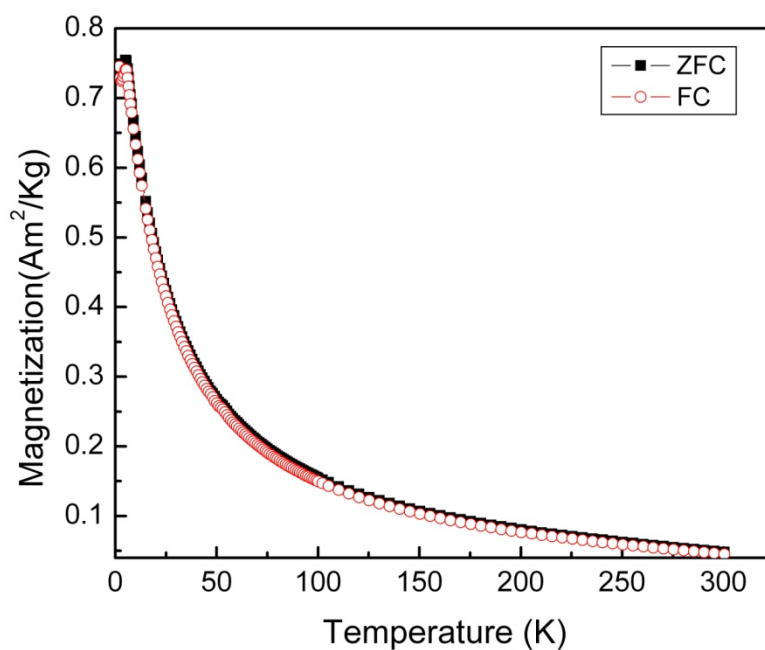


**Figure S12** Zero field cooling(ZFC) and field cooling (FC) curves.

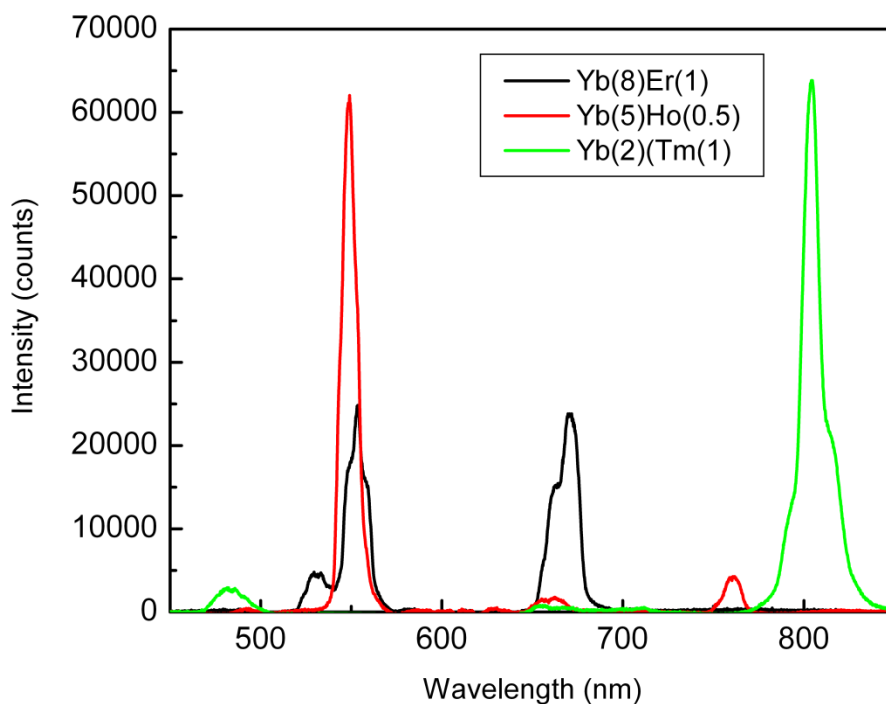


**Figure S13.** Comparison of the 980 nm excited upconversion emission spectral properties of  $Gd_2O_3$  doped with various concentration of Yb/Er, YbHo and YbTm.

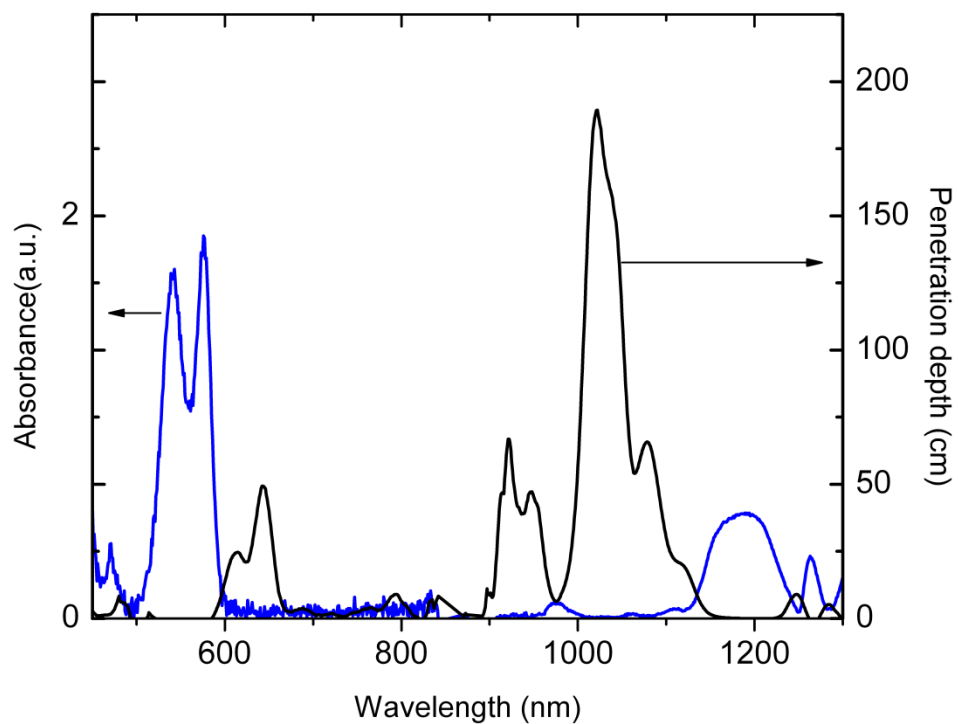


**Figure S14.** Absorption spectrum of pork muscle tissue and the calculated penetration depth spectrum. Penetration depth was calculated without considering the scattering components of the tissue.